

A finite element for viscothermal wave propagation

W.R. Kampinga, Y.H. Wijnant, A. de Boer

University of Twente, Structural Dynamics and Acoustics,
Institute of Mechanics, Processes and Control Twente
Drienerlolaan 5, P.O. Box 217, 7500 AE Enschede, The Netherlands
e-mail: w.r.kampinga@ctw.utwente.nl

Abstract

The well known wave equation describes isentropic wave propagation. In this equation, non-isentropic boundary layer effects are neglected. This is allowed if the characteristic dimensions of the acoustic domain are large with respect to the thickness of the boundary layers. However, in small acoustic devices such as hearing aid loudspeakers, the boundary layer effects are significant and can not be neglected. A model that describes viscothermal wave propagation is needed to model such devices.

For viscothermal wave propagation, the compressibility of air depends on the thermal behavior that can range from adiabatic to isothermal. Moreover, the propagation behavior can range from propagation with negligible viscosity to propagation with negligible inertia (Stokes flow). This complete range is accurately described by the *low reduced frequency model*. This model's major drawback is that it is only defined for simple geometries such as thin layers and narrow tubes. It is not valid for arbitrary geometries.

To overcome this drawback, a three dimensional viscothermal finite element has been developed. Like the LRF model, it covers the complete range from isothermal Stokes flow to isentropic acoustics. As opposed to the LRF model, the viscothermal finite element can be used to analyze complicated geometries.

This paper presents the weak formulation of the finite element. Furthermore, two examples are presented in which the results of the finite element models are compared to measurements.

1 Introduction

The response of miniature acoustic transducers, like hearing aid loudspeakers, is influenced by the viscosity and heat conduction of air. Therefore, these devices cannot be described by models based on standard isentropic acoustic equations. Unfortunately, not many models are available for viscothermal wave propagation. The low reduced frequency (LRF) model is an accurate option, but it is only defined for simple tube and layer geometries in which the wave propagation is effectively one dimensional or two dimensional; see Beltman [1]. The finite element presented in this paper is intended to model three dimensional viscothermal wave propagation, possibly in complicated geometries.

Viscothermal effects occur in boundary layers near walls. If these boundary layers are very small compared to the characteristic lengths of the geometry, it is usually possible to use isentropic acoustic models. In the other limit, when the geometry is much smaller than the boundary layer would be in open space, it is possible to use isothermal (compressible) Stokes flow models. In this limit, the fluid behavior cannot be called wave propagation anymore, because inertia is neglected. Nevertheless it is useful to think of viscothermal wave propagation as fluid behavior in between these two limits. Both the LRF model and the presented finite element is accurate for this complete range. Clearly, near either limit it is usually sensible to use a simplified model that describes this limit's behavior. Nevertheless, for the wide range in between these limits, the finite element for viscothermal wave propagation is a flexible, widely applicable modeling tool and a useful addition to LRF models.

Finite elements for viscothermal wave propagation have been published previously by Malinen [2] and Nijhof [3]. The element presented in this paper uses the same weak formulation as presented in Nijhof, but a different discretization. For completeness, a brief overview of the theory is presented in this paper. More details can be found in the mentioned references. The symbols used in this paper are listed in table 1.

| Symbol | Description | Value | Unit |
|----------------|---|-------------------------|----------------------------------|
| \mathbf{v} | Velocity vector | | m s^{-1} |
| T | Temperature perturbation | | K |
| p | Pressure perturbation | | Pa |
| ω | Angular frequency | | rad s^{-1} |
| τ | Viscous stress tensor | | Pa |
| κ | Heat conduction coefficient | 0.0254 | $\text{W m}^{-1} \text{K}^{-1}$ |
| ρ_0 | Quiescent density | 1.1859 | kg m^{-3} |
| T_0 | Quiescent temperature | 296.15 | K |
| p_0 | Quiescent pressure | 101325 | Pa |
| c_0 | Speed of sound | 345.8707 | m s^{-1} |
| C_p | Specific heat at constant pressure | 1009.6 | $\text{J kg}^{-1} \text{K}^{-1}$ |
| μ | Dynamic viscosity | $18.266 \cdot 10^{-6}$ | Pa s |
| λ | Second viscosity | $-1.2177 \cdot 10^{-6}$ | Pa s |
| δ_{bl} | Boundary layer thickness | | m |
| i | Imaginary unit | | |
| \mathbf{I} | Identity matrix | | |
| Ω | Domain | | m^3 (or m^2) |
| Γ | Boundary of domain Ω | | m^2 (or m) |
| ∇ | Gradient operator | | m^{-1} |
| Δ | Laplacian operator | | m^{-2} |
| \cdot | Inner product | | |
| $:$ | Double dot product | | |
| \mathbf{v}^T | Transpose of \mathbf{v} | | |
| \mathbf{v}^H | Conjugate transpose of \mathbf{v} | | |
| \mathbf{v}^t | test function corresponding to \mathbf{v} | | |

Table 1: Nomenclature, with used values

2 Theory

Viscothermal wave propagation is a subproblem of fluid dynamics which, under the continuum assumption, can be modeled by the Navier-Stokes equations. Constitutive behavior has been modeled by Fourier's law for heat conduction, the Newtonian fluid assumption for viscosity and the perfect gas laws for the equations of state. Finally, linearization and Fourier transformation lead to the set of equations (1) used for the finite element for viscothermal wave propagation. The set consists of the momentum equation (1a), the energy or enthalpy equation (1b) and the continuity equation (1c).

$$i\omega\rho_0\mathbf{v} - \nabla \cdot \tau + \nabla p = 0 \quad (1a)$$

$$i\omega\rho_0 C_p T - \kappa \Delta T - i\omega p = 0 \quad (1b)$$

$$\nabla \cdot \mathbf{v} - \frac{i\omega}{T_0} T + \frac{i\omega}{p_0} p = 0 \quad (1c)$$

The degrees of freedom (DOFs) are the components of the velocity vector \mathbf{v} , the temperature T and the pressure p . The terms with the viscous stress tensor τ and the heat conduction coefficient κ are responsible for

the viscothermal effects. Without these terms, the set of equations can be reduced to the acoustic Helmholtz equation. The viscous stress tensor τ is a function of the velocity DOFs:

$$\tau = \lambda (\nabla \cdot \mathbf{v}) \mathbf{I} + \mu (\nabla \mathbf{v} + (\nabla \mathbf{v})^T) \tag{2}$$

A weak formulation is created from the set of Navier Stokes equations (1) by multiplication with test functions \mathbf{v}^t , T^t and p^t respectively, followed by integration over the domain. Next, Stokes' divergence theorem is applied to the last two terms in the momentum equation and the second term in the enthalpy equation. This reduces all second order derivatives to first order derivatives and creates useful weak boundary terms (total force and heat flux). The resulting weak formulation is:

$$\int_{\Omega} (\tau : (\nabla \mathbf{v}^t) + i\omega\rho_0\mathbf{v} \cdot \mathbf{v}^t - p (\nabla \cdot \mathbf{v}^t)) \, d\Omega = \int_{\Gamma} (p + \tau \cdot \mathbf{n}) \cdot \mathbf{v}^t \, d\Gamma \tag{3a}$$

$$\int_{\Omega} (\kappa (\nabla T) \cdot (\nabla T^t) + i\omega\rho_0 C_p T T^t - i\omega p T^t) \, d\Omega = \int_{\Gamma} \kappa (\nabla T) \cdot \mathbf{n} T^t \, d\Gamma \tag{3b}$$

$$\int_{\Omega} \left(\nabla \cdot \mathbf{v} - \frac{i\omega}{T_0} T + \frac{i\omega}{p_0} p \right) p^t \, d\Omega = 0 \tag{3c}$$

Discretization of this set of weak equations yields the viscothermal finite element. Lagrange shape functions of second order are used for the velocity components, the temperature and their corresponding test functions (\mathbf{v} , \mathbf{v}^t , T and T^t), and Lagrange shape functions of first order are used for the pressure and the corresponding test functions (p and p^t). Using equal order shape functions for all DOFs would result in a unstable element. This finite element has a so called mixed formulation, because the continuity equation and the pressure DOF could have been eliminated from the set. The domain equations can be made symmetric but not Hermitian symmetric ($K = K^T \neq K^H$) by multiplication of the enthalpy equation (3b) with $-T_0^{-1}$ and the continuity equation (3c) with -1 . The natural boundary conditions then determine whether the complete system matrix becomes symmetric or not.

The total number of boundary conditions (BCs) that needs to be specified on each boundary is four: one thermal BC and three mechanical BCs (one in each direction). The thermal BC can be either temperature (essential), or heat flux (natural), and the mechanical BC can be either velocity (essential), or force (natural); see table 2. For example, a symmetry boundary is modeled with zero normal velocity, zero tangential forces (in two directions) and zero heat flux. Natural BCs can be an expression as function of the DOFs. This can be used to apply impedance BCs for example.

| Boundary condition | Weak equation | Essential | Natural |
|-----------------------|---------------|---------------------|---------------------------|
| Normal mechanical | Momentum (3a) | Normal velocity | Normal total force |
| Tangential mechanical | Momentum (3a) | Tangential velocity | Tangential viscous force* |
| Thermal | Enthalpy (3b) | Temperature | Heat flux |

* The tangential total force equals the tangential viscous force, because it is independent of the pressure.

Table 2: Applicable boundary conditions

3 Experimental validation

Results of viscothermal FEM calculations are compared to impedance tube measurements. The impedance tube, see figure 1(a), is a practical measurement device to calculate a sample's absorption coefficient at normal incidence. During the measurement, a broadband signal is applied to the speaker and the pressure

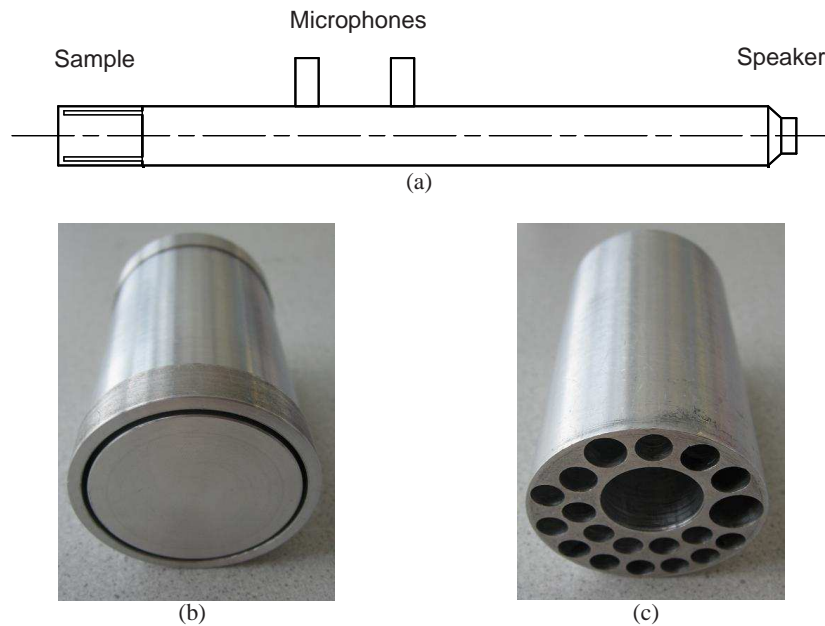


Figure 1: (a) Schematic overview of the impedance tube setup, (b) Photo of the cylindrical layer resonator, (c) Photo of the broadband resonator

perturbation is measured with two microphones. The absorption coefficient can be calculated from the two measurement signals and the known distance between the microphones.

Two samples were measured. Both are resonators that are influenced by viscothermal effects:

- a simple cylindrical layer resonator, optimized to reach an absorption coefficient of 1 at its resonance frequency, see figure 1(b)
- a more complicated broadband resonator with twenty tubes, see figure 1(c). It has been optimized by Hannink [5] for a high absorption coefficient between 1 and 2 kHz.

Both resonators were optimized using LRF models, which is possible because of the simple geometries involved. Clearly, the viscothermal finite element has been developed for more complicated geometries. Therefore, the presented experiments only serve as an experimental validation.

3.1 Cylindrical layer resonator

An axi-symmetrical viscothermal FEM model is used to model the cylindrical layer resonator shown in figure 1(b). The used FEM formulation is obtained by writing the weak form, equation (3), in cylinder coordinates. Next, the angular velocity, its test function and all angular derivatives are set equal to zero. Last, all remaining equations multiplied with the radial coordinate to prevent divisions by zero.

Figure 2(a) shows the FEM model. Only a small part of the impedance tube is modeled and the chamfers of the resonator are ignored. The impedance tube has a radius of 50 mm. The resonator's length is 70 mm, its layer thickness is 1 mm and its inner diameter is 42 mm. An adiabatic, unit normal force boundary condition is applied to the upper pressure measurement surface to excite the model. After solving the FEM problem, the absorption coefficient can be calculated from the pressures on the two pressure measurement surfaces.

Figures 2(b) and 2(c) show some post processing results at the plot area near the resonance frequency. The axial velocity profile changes near the outflow opening of the resonator. In figure 2(c), the radial velocity magnitude is shown. The line on which it is zero is curved to the nearby impedance tube wall. The dashed line in the plot clearly illustrates this effect.

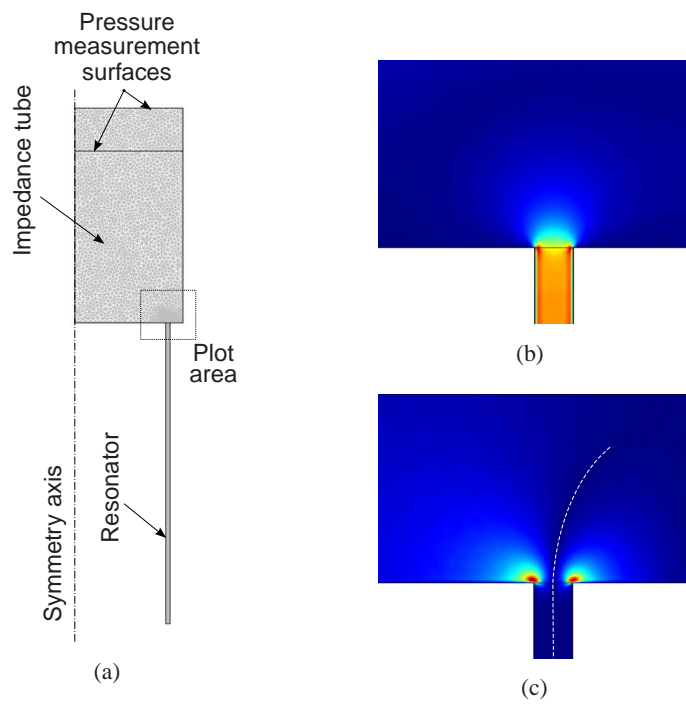


Figure 2: (a) Axi-symmetrical FEM model, (b) Magnitude of Axial velocity, (c) Magnitude of radial velocity

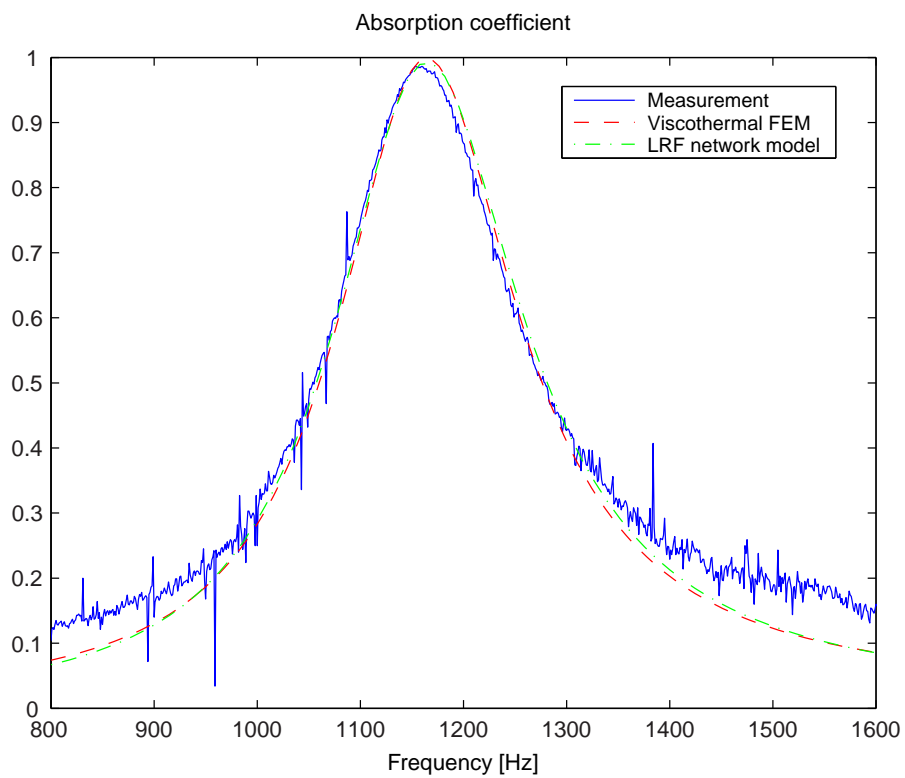


Figure 3: Absorption coefficient of the cylindrical layer resonator

The cylindrical layer resonator has a simple geometry that can be modeled by a one dimensional LRF network model; see Van der Eerden [4]. Such a model does not accurately describe the mentioned three dimensional effects near the outflow of the resonator. Nevertheless, these effects can be approximately modeled with an end correction. The well known acoustic end correction for baffled tubes is $\frac{8r}{3\pi}$ with r the tube radius. This tube radius can be expressed as twice the outflow surface area divided by the circumference length. Using the same reasoning for an infinitely long layer yields an end correction of $\frac{8h}{3\pi}$, with h the layer thickness¹. This end correction seems to work well in this case, because the estimated absorption coefficient of the cylindrical layer resonator corresponds well to the FEM model and to the measurement; see figure 3. Both the finite element and the LRF network model can describe this resonator accurately.

3.2 Broadband resonator

The broadband resonator shown in figure 1(c), is optimized for high absorption between 1 and 2 kHz; see Hannink [5]. An LRF network model was used to optimize the radii and lengths of the tubes. The optimized resonator was built using slightly different dimensions, for ease of manufacturing.

Figure 4 compares the measured response of the resonator to its LRF model with baffled tube end corrections and to its LRF model without end corrections. Although the models roughly match the measurements, neither is very accurate. This might have been expected, because the 3D outflow effects at the the open tube ends are not correctly taken into account in the LRF models; neither with baffled tube end corrections nor without end corrections. Inevitably, the outflow of a tube is affected by neighboring tubes, especially if the tube lengths are nearly equal. Therefore, standard end corrections can not be used. Likely, either a measurement or a FEM model is required to find accurate end corrections for this particular resonator. Perhaps an isentropic acoustic FEM model suffices, but this hypothesis has not been examined.

A three dimensional viscothermal FEM model was made of the resonator including a part of the impedance tube; see figure 6. This is a large model, especially because it contains many surfaces with boundary layers. The model contains 500,000 DOFs, even after some ideas to reduce the model size have been applied:

- The walls on which the viscothermal effects can be neglected are modeled with slip and adiabatic boundary conditions (identical to symmetry BC). These walls are the closed tube end surfaces and the surface of the impedance tube and they are blue in figure 6.
- The viscous boundary layer thickness is estimated as $\delta_v \approx \sqrt{\frac{\mu}{\rho_0 \omega}}$ and a somewhat larger boundary layer mesh is used in the tubes.

The results of the calculations are shown in figure 5. The absorption coefficient has been determined in a similar way as in the model of the cylindrical layer resonator. The FEM model is accurate for frequencies up to 1450 Hz, because it can accurately describe the three dimensional outflow effects of the tubes. The start and stop frequencies of the absorption range are also accurately predicted in the FEM model. Above 1450 Hz, the model only roughly corresponds to the measurement. Figure 5 also shows the results of a FEM calculation with a coarse mesh with 200,000 DOFs. The results above 1450 Hz are different, which indicates that the results have not completely converged to the solution of the underlying equations. Therefore, the original FEM model might be improved by using a finer mesh.

¹The viscothermal finite element can be used to calculate viscothermal baffled tube end corrections, or, better in this case, baffled layer end corrections. For simplicity, the mentioned end correction of $\frac{8h}{3\pi}$ has been used here.

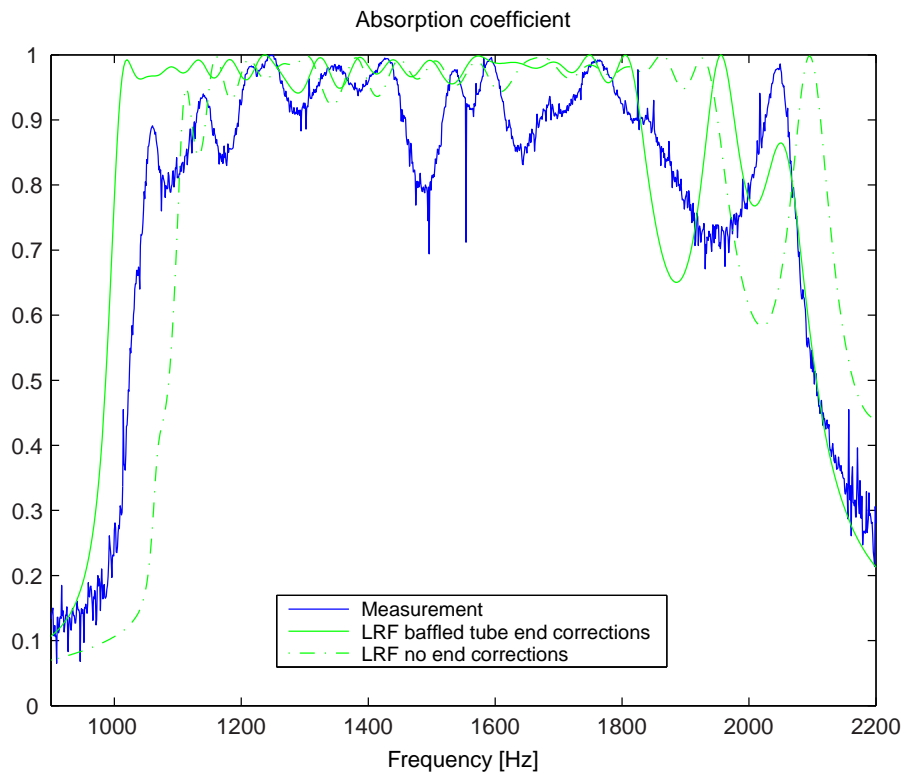


Figure 4: Absorption coefficient of the broadband resonator, LRF model

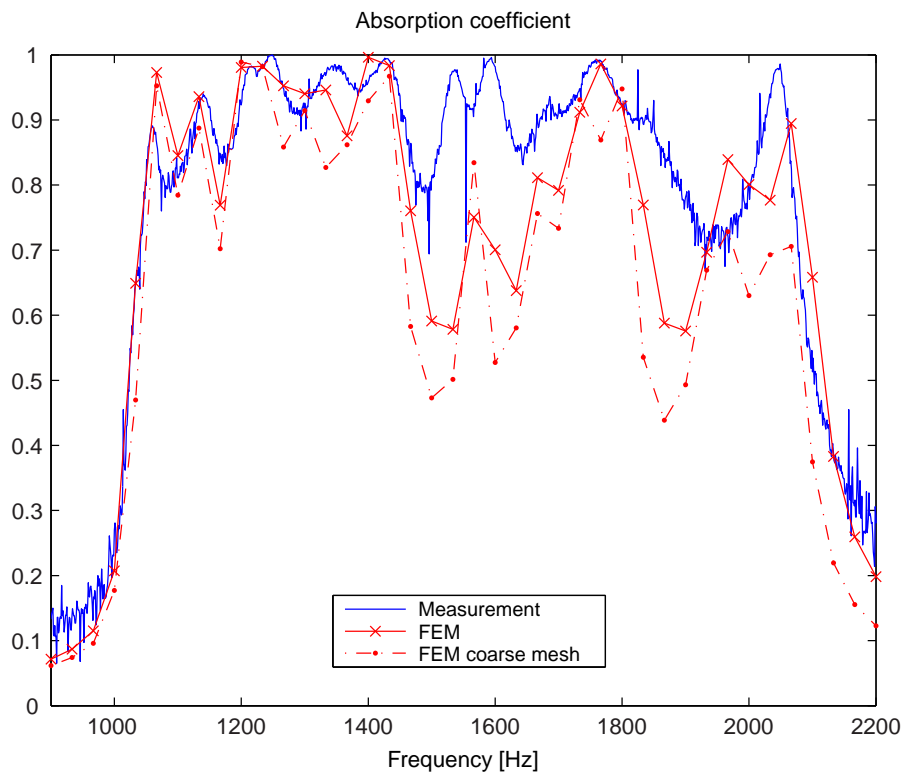


Figure 5: Absorption coefficient of the broadband resonator, FEM model

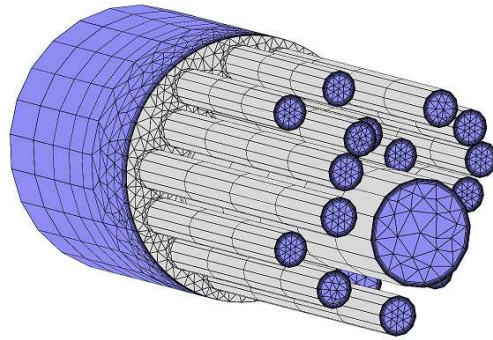


Figure 6: The broadband resonator model. The blue surfaces are modeled with adiabatic slip walls. The boundary layer mesh is visible at the tube ends.

4 Conclusion

A finite element for viscothermal wave propagation has been presented in this paper. It is intended to solve problems that cannot be modeled by the LRF model because of their complicated geometries. Examples of applications are miniature acoustic transducers and MEMS devices.

Impedance tube measurements of two samples were compared to the FEM calculations and the results match well. However, the limitation of the presented finite element in three dimensional problems is the required computer hardware. Careful meshing of three dimensional problems is required to reduce the problem size as much as possible.

Acknowledgements

The authors gratefully acknowledge *Sonion* for financing this research.

References

- [1] W.M. Beltman, *Viscothermal wave propagation including acousto-elastic interaction*, University of Twente, Applied Mechanics and Acoustics, Enschede (1998)
- [2] M. Malinen, M. Lyly, P. Råback, A. Kärkkäinen, L. Kärkkäinen, *A finite element method for the modeling of thermo-viscous effects in acoustics*, in *Proceedings of the European Congress on Computational Methods in Applied Sciences and Engineering, Jyväskylä, Finland, 2004 July 24-28, Jyväskylä* (2004).
- [3] M.J.J. Nijhof, Y.H. Wijnant, A. de Boer, *An acoustic finite element including viscothermal effects*, in *Proceedings of the 14th International Congress on Sound and Vibration, Cairns, Australia, 2007 July 9-12, Cairns* (2007).
- [4] F.J.M. van der Eerden, *Noise reduction with coupled prismatic tubes*, University of Twente, Applied Mechanics and Acoustics, Enschede (2000)
- [5] M.H.C. Hannink, Y.H. Wijnant, A. de Boer, *Optimized sound absorbing trim panels for the reduction of aircraft cabin noise*, in *Proceedings of the 11th International Congress on Sound and Vibration, St. Petersburg, Russia, 2004 July 5-8, St. Petersburg* (2004), pp. 1855-1862.